water

MDPI

Article

Adsorption–Desorption of Antimony (V) and Phosphorus (V) in Two Typical Soils: Release Behavior and Environmental Implications

Xingyu Lu [1], Yuting Zhao [1], Kefeng Yao [1], Fande Meng [1,2], Feiyue Li [1,2], Zhenyu Wu [1,2] and Yongbing Cai [1,2,*]

[1] College of Resource and Environment, Anhui Science and Technology University, Chuzhou 233100, China; luxingyu0218@163.com (X.L.); 19556956801@163.com (Y.Z.); yaokefeng0229@163.com (K.Y.); mengfd@ahstu.edu.cn (F.M.); lify@ahstu.edu.cn (F.L.); wuzy@ahstu.edu.cn (Z.W.)

[2] Anhui Province Agricultural Waste Fertilizer Utilization and Cultivated Land Quality Improvement Engineering Research Center, Chuzhou 233100, China

* Correspondence: caiyongbing0121@163.com

Abstract

The competitive adsorption between phosphorus (V) and antimony (V) may influence the release of antimony from Sb-contaminated soils. The objectives of this study were to evaluate the effect of P(V) on the adsorption–desorption behavior and transport of Sb(V) in two typical soil types. Specifically, the simultaneous adsorption, competitive interactions, and miscible displacement dynamics of P(V) and Sb(V) in these soils were investigated. Results clearly indicated that the competitive effect of P(V) on Sb(V) adsorption is more pronounced in acidic red soil than in alkaline calcareous soil. The adsorption capacity of Sb(V) decreased with increasing solution pH, leading to greater mobility of Sb(V) in both soils. P(V) was preferentially adsorbed over Sb(V) in both soil types. Sb(V) adsorption isotherms fitting by Freundlich model yielded higher coefficients of determination (R^2) compared to the Langmuir model, while the Langmuir model provided a good fit to the P(V) adsorption isotherms. The total released amounts of P(V) and Sb(V) accounted for 0% and 0.4%, respectively, in red soil and 2.7% and 48.6%, respectively, in calcareous soil, relative to their adsorption capacities. The red soil exhibited remarkably strong binding affinity, with only minimal amounts of P(V) and Sb(V) released after five consecutive desorption steps. Breakthrough curves (BTCs) revealed that the presence of P(V) can promote significant Sb(V) release from the soils, which persists over an extended duration. This study on the adsorption–desorption behavior of P(V) and Sb(V) in two typical soils enhances our understanding of their mobility, fate, and associated environmental risks. In conclusion, the assessment of environmental risks from antimony-contaminated soils should take into account the competitive adsorption–desorption interactions between Sb(V) and P(V).

Keywords: antimony; phosphorus; competitive adsorption; release; migration

check for updates

Academic Editor: Catherine N. Mulligan

Received: 16 September 2025
Revised: 9 October 2025
Accepted: 20 October 2025
Published: 22 October 2025

Citation: Lu, X.; Zhao, Y.; Yao, K.; Meng, F.; Li, F.; Wu, Z.; Cai, Y. Adsorption–Desorption of Antimony (V) and Phosphorus (V) in Two Typical Soils: Release Behavior and Environmental Implications. *Water* **2025**, *17*, 3038. https://doi.org/10.3390/w17213038

Copyright: © 2025 by the authors. Licensee MDPI, Basel, Switzerland. This article is an open access article distributed under the terms and conditions of the Creative Commons Attribution (CC BY) license (https://creativecommons.org/licenses/by/4.0/).

1. Introduction

Antimony (Sb) is widely utilized in various industrial applications due to its unique properties, including its use in flame retardants, brake pads, catalysts, and ammunition production [1,2]. However, as a toxic heavy metal, the extensive use of antimony and improper management of Sb-containing waste have led to significant environmental concerns [2–4]. Soil contamination by antimony poses serious threats to ecosystems and human health.

It not only endangers flora and fauna but also compromises water quality and enters the food chain, ultimately affecting humans [5]. Although antimony is not essential for plant growth, bioavailable Sb in soil can be absorbed by plant roots and accumulate within tissues [6]. Sb contamination can inhibit plant physiological processes such as photosynthesis, leading to toxicity [7]. Moreover, the accumulation of high concentrations of Sb in edible plant parts may pose severe health risks to humans, including immunological disorders, cardiovascular diseases, and even cancer [8].

Antimonate (Sb-V) and antimonite (Sb-III) are the two predominant forms of antimony in the natural environment, with Sb(V) being the dominant species in soils [9,10]. Although numerous studies have investigated the environmental behavior of Sb in minerals and soils, the fate and transport of Sb in soil systems remain poorly understood due to the inherent complexity and heterogeneity of soils. Previous research has extensively explored competitive adsorption between As/Sb [11–13] and As/P [14–17], primarily focusing on mineral surfaces. However, few studies have addressed the competitive adsorption–desorption between Sb and P, particularly in natural soil systems. Given that competitive adsorption can significantly influence the release of antimony from contaminated soils—thereby posing direct risks to water quality, crop safety, and ultimately human health [3]—there is a clear need for further research on the competitive adsorption behavior of phosphorus and antimony in soils.

Farmland soils receive phosphorus from various sources. A major input is the application of phosphate fertilizers to enhance soil phosphorus availability and improve crop yields. Intensive agricultural practices worldwide have led to the widespread use of phosphate fertilizers, with China being the largest producer globally [18]. At the same time, China accounts for over 80% of the world's antimony production [19,20], primarily concentrated in its southwestern regions. This has resulted in severe antimony contamination in local soils, with Sb levels reaching up to a thousand times higher than the natural background values [6]. Studies have shown that phosphate fertilizers can compete for adsorption sites in soils, which may increase the mobility and bioavailability of heavy metals such as arsenic in both agricultural and sediment environments [21–23]. Antimony, arsenic, and phosphorus all belong to Group VA in the periodic table and share similar chemical properties, including common oxidation states in environmental systems (ranging from -3 to +5) and an identical s^2p^3 outer electron configuration. Consequently, competitive adsorption between Sb and P is likely a critical factor influencing the release and transport of antimony in soils.

In China, the extensive mining of large amounts of antimony resources has led to a particularly prominent problem of soil antimony pollution. Therefore, the issue of antimony release from contaminated soil directly relates to the problem of food security and should be given attention. At present, there are relatively few studies on the competitive adsorption and desorption of antimony and phosphorus in natural soil systems. In this study, batch and column experiments were conducted to evaluate the influence of P(V) on the adsorption–desorption behavior and transport of Sb(V) in two typical soil types. The findings will contribute critical insights for assessing the fate, mobility, and environmental risks of Sb in contaminated sites.

2. Material and Methods

2.1. Soils

In this study, two soil samples with distinct physicochemical properties were collected from experimental stations under the Chinese Academy of Sciences: the Jiangxi Yingtan Farmland Ecosystem National Field Observation and Research Station and the Guangxi Huanjiang Farmland Ecosystem National Field Observation and Research Station. One

sample represents an acidic red soil (RS), while the other is an alkaline calcareous soil (CS). The fundamental physical and chemical properties of both soils are summarized in Table 1. Soil pH was determined by a pH meter (Metrohm 888 Titrando, Herisau, Switzerland) in a 1:10 (w/v) soil-water suspension following 30 min of stirring [24]. Total organic carbon (TOC) was measured using a total organic carbon analyzer (TOC-VCPH, Shimadzu Scientific Instruments, Kyoto, Japan). Concentrations of Fe and Al were quantified via ICP-MS (ELAN DRC II, Perkin Elmer SCIEX, Waltham, MA, USA) after digesting the soil samples. Particle size distribution was analyzed with a laser diffraction particle size analyzer (Mastersizer 2000F, Marlvern Instruments, Malvern, UK). These two soils were selected due to their contrasting acid–base characteristics, which are representative of the major soil types found in the antimony-producing regions of southwestern China. All chemicals used in this study were of analytical grade or higher.

Table 1. Selected physical and chemical properties of the studied soils.

Soil	pH	TOC [1] (g kg^{-1})	CEC [2] (cmol kg^{-1})	Total Fe (g kg^{-1})	Total Al (g kg^{-1})	Sand [3] (%)	Silt (%)	Clay (%)
RS	4.8	2.1	16	26	13	31	54	14
CS	7.4	25	25	52	22	33	49	16

Note(s): [1] TOC = total organic carbon. [2] CEC = cation exchange capacity. [3] Grain size distribution: sand (2.00–0.05 mm), silt (0.05–0.002 mm), clay (<0.002 mm).

2.2. Batch Experiments

To examine the potential influence of phosphate on antimony adsorption in the two soils, a series of experiments were conducted with a fixed antimony concentration and varying phosphate levels. A solid–liquid ratio of 1:10 was maintained by adding 3.0 g of soil to 30 mL of solution containing both phosphate and antimony in 50 mL centrifuge tubes. The initial P(V) concentrations ranged from 0.1 to 10 mM (0.1, 0.5, 1, 5, and 10 mM), while the Sb(V) concentration was held constant at 1 mM. The mixtures were shaken at 200 rpm for 24 h, then centrifuged to separate the solid and liquid phases. A 10 mL aliquot of the supernatant was collected and filtered prior to analysis. The P(V) and Sb(V) solutions were prepared using KH_2PO_4 and $KSb(OH)_6$, respectively. To maintain a constant ionic strength, 0.01 M $KClO_4$ was used as the background electrolyte. All chemicals were of analytical grade, and all experiments were performed in triplicate.

Equilibrium sorption isotherms were obtained through batch experiments conducted at room temperature under aerobic conditions. For each sample, 3.0 g of soil was weighed into a 50 mL centrifuge tube, followed by the addition of 30 mL of solution containing specified concentrations of P and Sb. The mixtures were shaken at 200 rpm for 24 h and then centrifuged to separate the solid and liquid phases. A 10 mL aliquot of the supernatant was collected and filtered for subsequent analysis. The isothermal adsorption experiments included three treatment groups: phosphate alone, antimony alone, and a mixed solution of phosphate and antimony. All experiments were performed in triplicate. The specific concentrations of phosphate and antimony used in each treatment are provided in Table 2.

Kinetic batch experiments were performed to examine the time-dependent adsorption–desorption behavior and dynamic competition between P(V) and Sb(V), using initial concentrations of 1 mM P(V) and 0.16 mM Sb(V). For each replicate, 3.0 g of soil was weighed into a 50 mL centrifuge tube, and 30 mL of the mixed P(V) and Sb(V) solution at the specified concentrations was added. The tubes were oscillated at 200 rpm in a constant-temperature shaker. Samples were collected after reaction times of 0.5, 1, 3, 6, 12, 24, and 48 h, followed by centrifugation. A 1 mL aliquot of the supernatant was then diluted to 10 mL for subsequent analysis. The adsorbed amounts of P(V) and Sb(V) were calculated based on the difference between the initial and final concentrations. Desorption

was quantified immediately after the final adsorption step using the same batch system. The supernatant was replaced with 30 mL of 0.01 M $KClO_4$ background solution, and the mixture was shaken for 24 h. After centrifugation, 10 mL of the supernatant was collected and filtered for analysis. The desorption process was repeated five times, resulting in a total experimental duration of 120 h. All experiments were conducted in triplicate.

Table 2. The specific concentrations of P(V) and Sb(V) in the solutions.

Groups	P(V) (mM)	Sb(V) (mM)
Single phosphate solution	1, 2, 5, 10, 20	0
Single antimony solution	0	0.1, 0.5, 1, 5, 10
Phosphate and antimony mixed solution	1, 2, 5, 10, 20	0, 1, 5
Phosphate and antimony mixed solution	0, 1, 5	0.1, 0.5, 1, 5, 10

2.3. Models

The adsorption equilibrium data were modeled using the Freundlich and Langmuir isotherm equations. The Freundlich equation is expressed as $Q = K_F C^N$, where Q represents the equilibrium adsorption capacity, K_F is the Freundlich distribution coefficient, N denotes the nonlinear reaction order, and C is the equilibrium concentration. The Langmuir equation is given by $Q = Q_{\max} \frac{K_L C}{1+K_L C}$, where Q is the equilibrium adsorption capacity, $Q_{\max}$ is the maximum adsorption capacity, K_L is the Langmuir affinity coefficient, and C represents the equilibrium concentration.

2.4. Column Experiments

Acrylic columns (8.5 cm in length and 2.5 cm internal diameter) were uniformly packed with soil and slowly saturated with a background solution of 0.01 M $KClO_4$ under a low Darcy flux. Solutions were then introduced into each soil column at a constant flow rate using a peristaltic pump. A desorption phase was initiated by switching the input to either the background solution or a solution containing competing ions, delivered at the same flow rate. Three experimental treatments were established: (1) Input of a mixed phosphate–antimony solution [0.16 mM Sb(V) and 1 mM P(V)]; (2) Input of phosphate solution only [1 mM P(V)]; (3) Input of antimony solution only [0.16 mM Sb(V)]. The corresponding desorption solutions consisted of: (1) Background solution (0.01 M $KClO_4$); (2) Antimony solution [0.16 mM Sb(V)]; (3) Phosphate solution [1 mM P(V)]. Effluent samples were collected automatically at 1 h intervals.

2.5. Sample Analysis

The concentration of Sb(V) was determined using Hydride Generation Atomic Fluorescence Spectrometry (HG-AFS; Jitian Instrument Co., Beijing, China). The concentration of P(V) was quantified by Inductively Coupled Plasma Optical Emission Spectrometry (ICP-OES; Perkin Elmer SCIEX, Waltham, MA, USA).

2.6. Data and Figure Processing

Data processing, statistical analysis, and graphical representation were conducted using Microsoft Excel 2021 and Origin 2015 (OriginLab Corporation, Northampton, MA, USA).

3. Results and Discussion

3.1. Effect of P(V) on Sb(V) Adsorption

To investigate the effect of P(V) on the adsorption behavior of Sb(V) in two contrasting soil types, equilibrium adsorption experiments were conducted under conditions where

the Sb(V) concentration remained constant while that of P(V) was varied. The results are presented in Figure 1. In the absence of P(V), the adsorption capacity of Sb(V) was significantly higher in the acidic red soil than in the alkaline calcareous soil. However, as the P(V) concentration increased, this difference gradually diminished. At a P(V) concentration of 10 mM, the Sb(V) adsorption capacity in the acidic red soil became lower than that in the alkaline calcareous soil. These results indicate that P(V) concentration is a key factor influencing the adsorption behavior of Sb(V) in these soils. When both P(V) and Sb(V) are present in solution, P(V) is preferentially adsorbed over Sb(V), demonstrating a competitive adsorption advantage. Furthermore, it can be concluded that soil type also serves as an important factor affecting the adsorption of P(V) and Sb(V) [25].

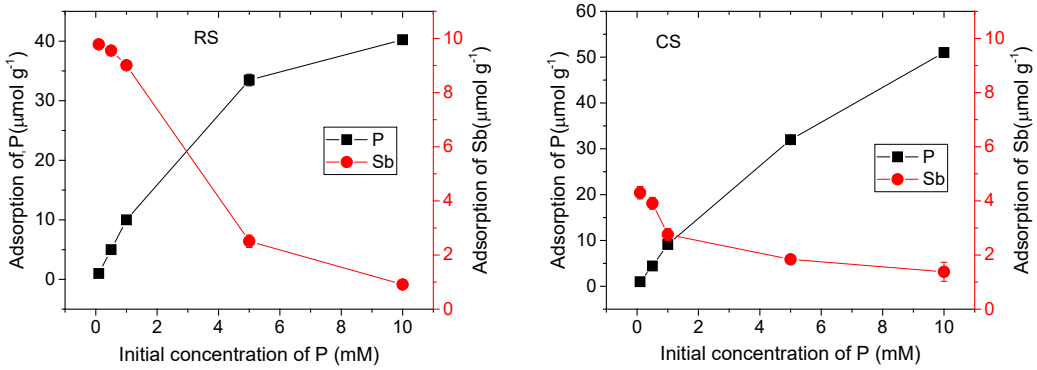


Figure 1. Effect of P(V) on adsorption of Sb(V) in red soil (RS) and calcareous soil (CS).

As the concentration of P(V) in the solution increased, the adsorption capacity of Sb(V) decreased significantly in both soils. Specifically, the Sb(V) adsorption capacity declined from 9.78 μmol·g^{-1} to 0.91 μmol·g^{-1} in the red soil, and from 4.30 μmol·g^{-1} to 1.38 μmol·g^{-1} in the alkaline calcareous soil. This reduction can be attributed to the competitive adsorption between P(V) and Sb(V) for binding sites on soil particle surfaces. The competitive effect of P(V) was more pronounced in the acidic red soil than in the alkaline calcareous soil. Additionally, the increase in P(V) concentration may also alter the pH of the soil solution, which is a key factor influencing Sb adsorption [26–28]. Therefore, when evaluating the competitive adsorption behavior of P(V) and Sb(V), it is essential to also consider concomitant changes in soil solution pH.

3.2. Adsorption Isotherm

To evaluate the influence of solution pH on the adsorption of P(V) and Sb(V) in soils, the final pH values from the isothermal adsorption experiments were analyzed (Figure 2). Due to variability in pH changes across treatments, results are reported based on the final pH rather than the initial pH [28]. In the alkaline calcareous soil, the equilibrium solution pH remained relatively stable following the addition of P(V) and Sb(V). In contrast, the equilibrium pH in the acidic red soil increased with rising concentrations of P(V) and Sb(V), with P(V) exerting a more pronounced effect on pH alteration. These observations indicate that the final solution pH is co-determined by the intrinsic soil properties and the concentrations of P(V) and Sb(V). The alkaline calcareous soil, characterized by weak alkalinity (pH 7.4), high total organic carbon (TOC, 25 g·kg^{-1}), and high cation exchange capacity (CEC, 25 cmol·kg^{-1}) (Table 1), exhibited strong buffering capacity, thereby minimizing fluctuations in equilibrium pH upon the introduction of antimony and phosphate. In comparison, the acidic red soil, with lower initial pH, TOC, and CEC values (Table 1), demonstrated limited buffering ability, leading to more significant variations in equilibrium solution pH in response to P(V) and Sb(V) additions.

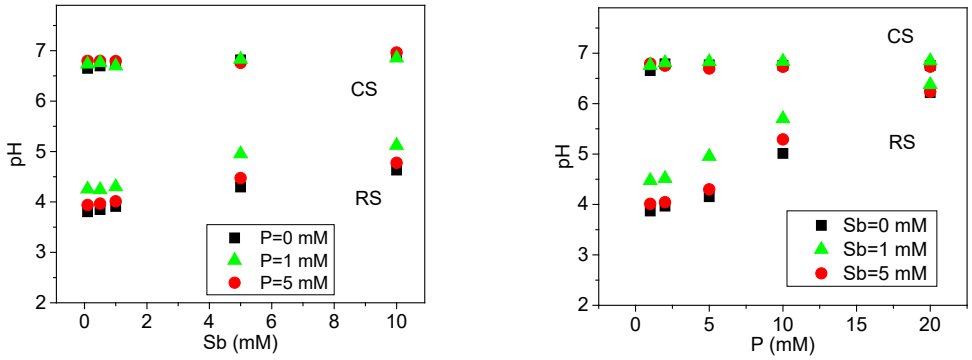


Figure 2. Equilibrium solution pH of Sb(V)/P(V) isothermal adsorption in acidic red soil (RS) and alkaline calcareous soil (CS).

Figure 1 presents the equilibrium adsorption isotherms of Sb(V) and P(V) in the red soil and calcareous soil. The best-fit parameters and goodness-of-fit statistics for the three initial concentrations of competing ions are summarized in Table 3. Within the experimental equilibrium concentration range, the adsorbed amount of Sb(V) did not reach saturation under the conditions studied (Figure 3A,B). The Freundlich model yielded higher coefficients of determination (R^2) compared to the Langmuir model, particularly in the acidic red soil (Table 3). The Freundlich parameter N is commonly interpreted as an indicator of surface energy heterogeneity, reflecting variability in sorption affinities and the potential for multilayer adsorption [29,30]. The Sb(V) adsorption isotherms (Figure 3A,B) demonstrate clear nonlinear behavior in both soils, with notably low values of the nonlinear exponent N (ranging from 0.389 to 0.444) in the red soil. These low N values suggest strong concentration-dependent sorption, where high-energy sites are preferentially occupied at low solution concentrations. This behavior aligns with previously reported Sb(V) isotherms at low equilibrium concentrations (below 800 μmol·L^{-1}) [26]. The suppression of Sb(V) adsorption in the presence of P(V) (Figure 3A,B) further indicates that the adsorption sites are not specific to Sb(V), consistent with the competitive interaction observed between P(V) and Sb(V) in both soil types.

Table 3. Estimated Freundlich and Langmuir parameters for Sb(V) and P(V) adsorption isotherms in acidic red soil (RS) and alkaline calcareous soil (CS).

Element	Soil	Treatment	Langmuir			Freundlich		
			Q_{max} (μmol/g)	$1/K_L$ (μmol/L)	R^2	K_F (μmol g^{-1})/[(μmol $L^{-1})^{1/n}$])	N	R^2
Sb	RS	P = 0 mM	114.9	939.4	0.97	3.926	0.39	0.99
		P = 1 mM	55.31	101.6	0.98	3.011	0.41	1
		P = 5 mM	46.95	292.6	0.98	1.455	0.44	1
	CS	P = 0 mM	107.4	5176	0.99	0.076	0.77	1
		P = 1 mM	129.8	9129	1	0.038	0.83	1
		P = 5 mM	204.7	24,355	0.99	0.011	0.94	0.98
P	RS	Sb = 0 mM	51.06	22.08	0.99	13.45	0.15	0.82
		Sb = 1 mM	46.96	29.24	0.94	12.06	0.16	0.92
		Sb = 5 mM	44.74	94.74	0.96	8.398	0.19	0.89
	CS	Sb = 0 mM	64.73	513.9	0.91	5.69	0.26	0.98
		Sb = 1 mM	59.63	642.5	0.81	4.47	0.28	0.99
		Sb = 5 mM	55.44	636.9	0.92	3.75	0.29	0.98

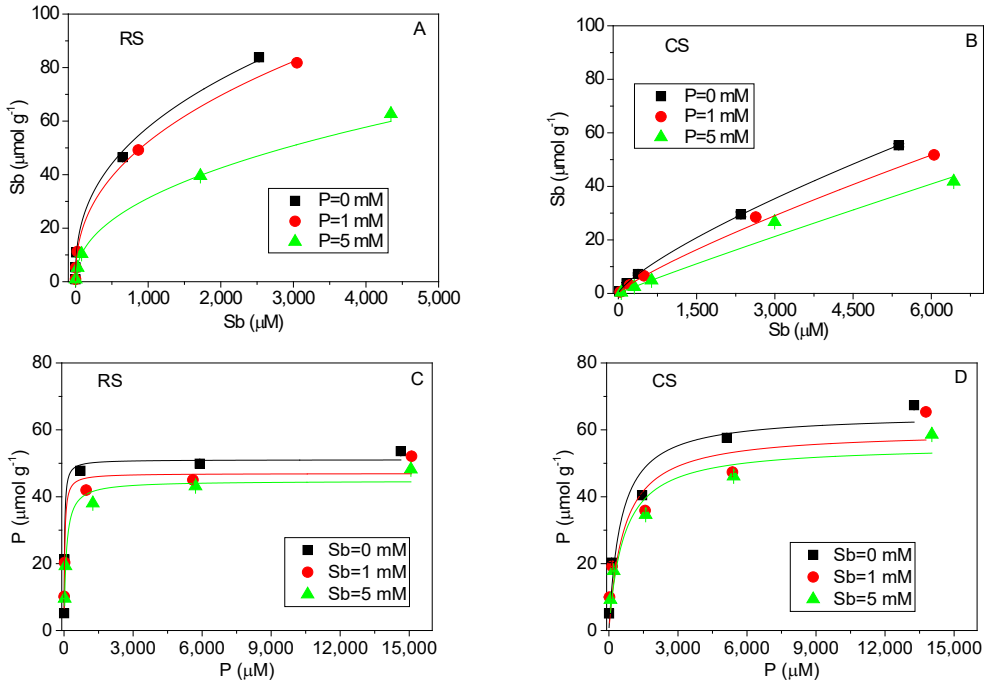


Figure 3. Equilibrium isotherms of Sb(V) and P(V) adsorption in acidic red soil (RS) and alkaline calcareous soil (CS). (**A**,**B**): Sb(V) adsorption isotherms with solid lines fitting by Freundlich equation. (**C**,**D**): P(V) adsorption isotherms with solid lines fitting by Langmuir equation.

The adsorption isotherms of P(V) in the presence of Sb(V) for both soils are shown in Figure 3C,D. The Langmuir model provided a good fit to the experimental data, particularly in the acidic red soil, indicating that P(V) adsorption occurs primarily on specific homogeneous sites in this soil type [31]. In contrast to Sb(V), the adsorption of P(V) was only marginally influenced by the presence of Sb(V). This phenomenon may be attributed to several factors. First, both common and element-specific adsorption sites likely coexist on the soil surfaces. In the acidic red soil, where the solution pH is relatively low (Figure 2), P(V) adsorption is likely dominated by specific sites, thereby reducing its susceptibility to competitive displacement [28]. Second, previous studies have indicated that Sb(V) tends to form monodentate complexes, whereas P(V)—similar to As(V)—can form more stable bidentate complexes [32]. Since bidentate complexes occupy more binding sites and achieve surface saturation more readily, the presence of P(V) leads to a pronounced decrease in Sb(V) adsorption with increasing P(V) concentration.

3.3. Kinetic Sorption-Desorption

The pH variations during the sorption–desorption kinetics of Sb(V) and P(V) in the acidic red soil (RS) and alkaline calcareous soil (CS) are shown in Figure 4. Over time, the solution pH in both soils decreased slightly and stabilized after approximately 24 h, remaining constant until the final sampling. Compared to the pronounced pH changes observed under higher concentrations of P and Sb (Figure 2), the lower concentration treatment [0.16 mM Sb(V) and 1 mM P(V)] had a minimal influence on the solution pH. Under these conditions, the pH was predominantly governed by the intrinsic soil properties (Table 1, Figure 4), particularly in the RS soil, as evidenced by the comparative results in Figures 2 and 4.

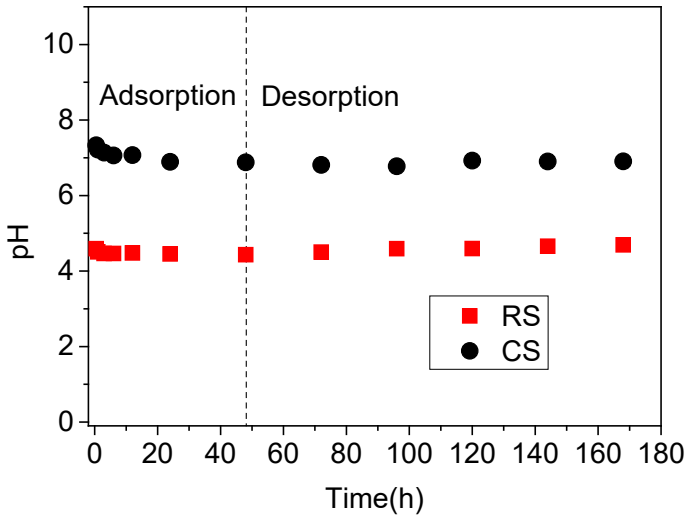


Figure 4. The pH of the solution during sorption-desorption kinetics of Sb(V) and P(V) in acidic red soil (RS) and alkaline calcareous soil (CS). The experiments were performed by mixing 3.0 g soil with 30 mL Sb(V) (0.16 mM) and P(V) (1 mM) mixed solution prepared in 0.01 M $KClO_4$.

The time-dependent adsorption–desorption behaviors of Sb(V) and P(V) in acidic red soil (RS) and alkaline calcareous soil (CS) are shown in Figure 5. The results indicate that the adsorption kinetics of both P(V) and Sb(V) were significantly faster in RS than in CS, reflecting the influence of contrasting soil properties. A notable observation is that the adsorption rates of P(V) and Sb(V) decrease with increasing solution pH, with P(V) exhibiting a particularly pronounced sensitivity to pH variation. This trend aligns with the kinetic study of As(III/V) adsorption on goethite by Waltham and Eick [33], which reported maximum adsorption rates near the respective pKa_1 values of the oxyanions. Antimony, arsenic, and phosphorus share similar geochemical characteristics due to their identical outer electron configuration (s^2p^3) and common oxidation states (−3 to +5) in environmental systems. The affinity of antimonate (pKa_1 = 2.72) and phosphate (pKa_1 = 2.12) for soil surfaces is expected to be highest under acidic conditions and to decline as pH increases. The adsorption kinetics of P(V) were considerably faster than those of Sb(V): P(V) reached equilibrium almost immediately in red soil and within 12 h in calcareous soil, whereas Sb(V) did not attain equilibrium in the calcareous soil even after 48 h. This slow adsorption kinetics of Sb(V) in calcareous soil is consistent with previous studies reporting that Sb(V) sorption may require several days to reach equilibrium [34].

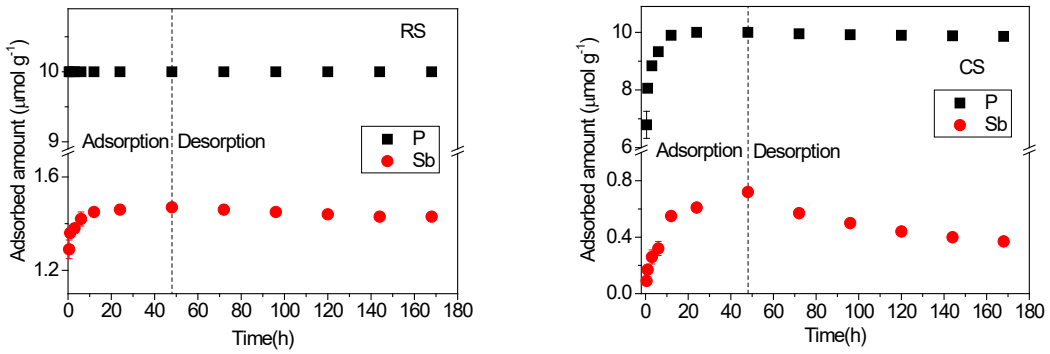


Figure 5. Adsorption–desorption kinetics of Sb(V) and P(V) in acidic red soil (RS) and alkaline calcareous soil (CS). The experiments were performed by mixing 3.0 g soil with 30 mL Sb(V) (0.16 mM) and P(V) (1 mM) mixed solution prepared in 0.01 M $KClO_4$.

All P(V) in the solution was adsorbed by the RS soil at the first sampling time and by the CS soil within 12 h. In contrast, the adsorbed amounts of Sb(V) at 48 h were 1.47 μmol·g^{-1} in RS soil and 0.72 μmol·g^{-1} in CS soil. These values are notably lower than those reported for Sb(V) adsorption in the absence of P(V) under identical experimental conditions [26]. The results clearly indicate that P(V) significantly inhibits Sb(V) sorption in both soils, reflecting a competitive interaction analogous to that observed between P(V) and As(V) [35]. These kinetic findings are consistent with the competitive behavior previously identified in equilibrium studies (Figures 1 and 3). P(V) was more effectively adsorbed than Sb(V) in both soils within the binary system. This can be attributed to differences in their acid dissociation properties and molecular structures. Phosphoric acid (H_3PO_4) undergoes successive deprotonation ($pKa_1 = 2.12$; $pKa_2 = 7.21$; $pKa_3 = 12.67$), enabling P(V) species such as HPO_4^{2-} to carry higher negative charges under environmental conditions. In comparison, antimonic acid (H_3SbO_4) dissociates only once ($pKa \approx 2.72$), predominantly forming $H_2SbO_4^-$ [2]. The greater negative charge of P(V) oxyanions likely requires stronger electrostatic interaction with positively charged surface sites, enhancing its adsorption affinity. Additionally, Sb(V) forms octahedral complexes with oxygen, resulting in a larger molecular structure than the tetrahedrally coordinated P(V), which may further contribute to the weaker adsorption of Sb(V) relative to P(V) [12].

As shown in Figure 5, the total released amounts of P(V) and Sb(V) accounted for 0% and 0.4% of the adsorption capacity in the RS soil, and 2.7% and 48.6% in the CS soil, respectively. The RS soil exhibited remarkably strong binding affinity, with only minimal amounts of P(V) and Sb(V) released even after five consecutive desorption steps. In contrast, P(V) was predominantly adsorbed onto high-energy sites in the CS soil, whereas a substantial fraction of Sb(V) was retained on low-energy sites. This observation aligns with the adsorption kinetics of the two elements: adsorption on high-energy sites occurs rapidly, while retention on low-energy sites is slower. Consequently, Sb(V) did not reach adsorption equilibrium in the CS soil within 48 h (Figure 5), and its sorption isotherm exhibited an approximately linear trend (Figure 3). The results further indicate that Sb(V) adsorption increases at higher input concentrations, primarily through accumulation on low-energy sites. McComb et al. [36] reported that Sb(V) is released more rapidly at higher pH from iron oxides due to decreased sorption affinity. Thus, the contrasting pH values of the two soils may contribute significantly to the differences in P(V) and Sb(V) desorption kinetics. Moreover, the total amount of Sb(V) released in the presence of P(V) was substantially higher than that in its absence under identical experimental conditions [26]. This finding supports the competitive effect of phosphate on the desorption and release of Sb [37] and As [38]. The presence of P(V) occupies a portion of the high-energy adsorption sites, thereby reducing the availability of such sites for Sb(V) and forcing more Sb(V) to adsorb onto low-energy sites. As a result, a greater proportion of Sb(V) becomes susceptible to desorption and release from the soil.

3.4. Non-Equilibrium Transport

The breakthrough curves (BTCs) of P(V) and Sb(V) in soil columns of acidic red soil (RS) and alkaline calcareous soil (CS) are presented in Figure 6 to illustrate their competitive transport behavior. When the input solution consisted of a mixed phosphate–antimony solution [0.16 mM Sb(V) and 1 mM P(V)], the BTCs for both P(V) and Sb(V) in the RS soil exhibited significant retardation, with breakthrough initiating after approximately 50 pore volumes and gradually reaching full breakthrough ($C/C_0 = 1$) after about 150 pore volumes. In contrast, the BTCs for the CS soil showed earlier and faster breakthrough, reaching relative concentrations (C/C_0) of 0.3–0.5 within fewer pore volumes, and attaining full breakthrough after approximately 200 pore volumes. These results align with findings

from kinetic sorption experiments, indicating a lower adsorption rate for both P(V) and Sb(V) in the CS soil. A sharp decline in effluent concentrations of P(V) and Sb(V) was observed upon switching the input solution from the mixed P(V)–Sb(V) solution to the background electrolyte (0.01 M $KClO_4$), particularly in the RS soil. Only a small amount of P(V) and Sb(V) was released from the CS soil, which is also consistent with the kinetic sorption results, further underscoring the stronger retention and competitive adsorption dynamics in the RS soil.

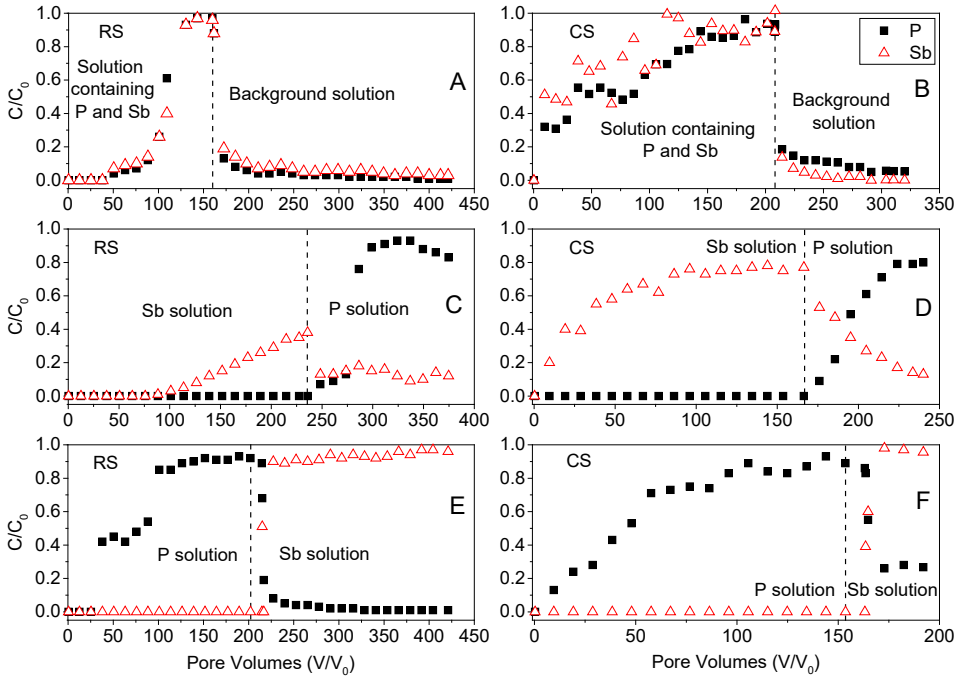


Figure 6. Breakthrough curves (BTCs) of Sb(V) and P(V) from soil columns. Symbols are experiment observations and dashed lines indicate desorption start times. (**A**,**B**): Input solution is phosphate antimony mixed solution [0.16 mM Sb(V) and 1 mM P(V)], desorption solution is background solution (0.01 M $KClO_4$). (**C**,**D**): Input solution is antimony solution [0.16 mM Sb(V)], desorption solution is phosphate solution [1 mM P(V)]. (**E**,**F**): Input solution is phosphate solution [1 mM P(V)], desorption solution is antimony solution [0.16 mM Sb(V)].

Figure 6C,D presents the breakthrough curves (BTCs) for the scenario where the input solution contained 0.16 mM Sb(V) and the desorption solution consisted of 1 mM P(V). The breakthrough of Sb(V) in the RS soil column exhibited pronounced retardation, commencing after approximately 100 pore volumes—a longer delay compared to the treatment with the mixed P(V)–Sb(V) solution. This further supports the inhibitory effect of P(V) on Sb(V) adsorption in soils. After applying about 240 pore volumes of Sb(V) solution to the RS column, the peak Sb(V) concentration in the leachate reached approximately 40% of the input concentration. Subsequent introduction of the 1 mM P(V) desorption solution induced sustained release of Sb(V) from the RS column, with effluent concentrations around 10% of the input level over an extended period. The BTCs for the CS soil displayed a distinctly different shape from those of the RS soil, reflecting fundamental differences in soil properties. Shangguan et al. [25] also reported varying Sb migration patterns across four soil types, with Sb mobility decreasing in the order: Sandy soil > Primosol > Isohumosol > Ferrosol. In contrast, Zhang et al. [26] observed longer retardation and lower peak concentrations ($C/C_0 < 0.12$ for acidic red soil; $C/C_0 < 0.55$ for alkaline calcareous soil) than those in the present study. This discrepancy may be attributed to differences in leaching concentration and soil structural characteristics resulting from column packing methods, as demonstrated in column percolation tests [39]. The introduction of P(V) solution prompted

substantial Sb(V) release from both soils, indicating that kinetic sorption processes in column experiments are more pronounced than in batch systems. In conclusion, as a key geochemical factor, the competing anion P(V) significantly influences the adsorption–desorption and transport behavior of antimony in soils, thereby affecting its migration and transformation within the vadose zone.

The solution flow sequence in Figure 6E,F involved the initial application of 1 mM P(V), followed by 0.16 mM Sb(V). The extended gradual increase in relative concentration (C/C_0) to full breakthrough ($C/C_0 = 1$) after approximately 200 pore volumes of P(V) solution indicates non-equilibrium or time-dependent retention of P(V). A sharp decline in P(V) concentration and a brief, transient breakthrough of Sb(V) were observed immediately after switching the input solution from 1 mM P(V) to 0.16 mM Sb(V), particularly in the RS soil column. This suggests that nearly all adsorption sites were occupied by P(V), making it difficult for Sb(V) to compete for these sites. In the calcareous CS soil, the replacement of the solution resulted in partial release of P(V), likely attributable to its earlier adsorption onto lower-energy sites—a behavior consistent with the kinetic sorption-desorption experiments.

In this study, we demonstrate that the interactions between P(V) and Sb(V) in two typical soils are significant and complex, substantially influencing the kinetic sorption-desorption behavior and transport of Sb(V). An important finding is that not only the sorption capacity of Sb(V), but also its sorption kinetics, are affected by factors such as the sequence of solution introduction and the method of soil column packing. The presence of P(V) can induce considerable and prolonged release of Sb(V) from soils, highlighting the necessity to incorporate these competitive dynamics into environmental risk assessments and the management of phosphate fertilizer applications in Sb-contaminated areas.

4. Conclusions

The results indicate that the competitive adsorption effect of P(V) on Sb(V) is more pronounced in acidic red soil than in alkaline calcareous soil. Kinetic sorption experiments further confirm that P(V) is adsorbed more effectively than Sb(V) in both soil types. The presence of P(V) significantly enhanced the release of Sb(V), with the total amount desorbed substantially higher in systems containing P(V) compared to those without. Column experiments revealed that the introduction of P(V) resulted in considerable and prolonged release of Sb(V), underscoring the necessity to account for such interactions in environmental risk assessments and phosphate fertilizer management at Sb-contaminated sites. This study elucidates the competitive adsorption–desorption dynamics between Sb(V) and P(V) and emphasizes the critical role of P(V) in facilitating Sb(V) release and migration in contrasting soil types. The competitive adsorption and desorption of Sb(V) and P(V) in the soil are influenced by various factors, including soil properties (pH, TOC, CEC), the main forms of Sb(V) and P(V), and their chemical structures. Consequently, comprehensive evaluation of environmental risks from antimony-contaminated soils must incorporate the competitive adsorption–desorption behavior of Sb(V) and P(V). In agricultural production, it is recommended to reduce the application of phosphorus fertilizers in soil contaminated by antimony.

Author Contributions: X.L.: Conceptualization, original draft, and validation. Y.Z.: Resources, investigation, visualization. K.Y.: Investigation, visualization, formal analysis. F.M.: Resources, visualization. F.L.: Investigation, visualization, funding acquisition. Z.W.: Investigation, visualization. Y.C.: Project administration, funding acquisition, writing—review and editing. All authors have read and agreed to the published version of the manuscript.

Funding: This work was financially supported by the National Natural Science Foundation of China (41907137), University Natural Science Research Project of Anhui Province (2023AH051860), Outstand-

ing Youth Scientific Research Project of Universities in Anhui Province (2022AH020089), and Innovation and Entrepreneurship Training Program for College Students, Anhui, China (S202410879285).

Data Availability Statement: Data will be made available on request.

Conflicts of Interest: The authors declare that they have no known competing financial interests or personal relationships that could have appeared to influence the work reported in this paper.

References

1. Filella, M.; Belzile, N.; Chen, Y. Antimony in the environment: A review focused on natural waters I. Occurrence. *Earth-Sci. Rev.* **2002**, *57*, 125–176. [CrossRef]
2. Wilson, S.; Lockwood, P.; Ashley, P.; Tighe, M. The chemistry and behaviour of antimony in the soil environment with comparisons to arsenic: A critical review. *Environ. Pollut.* **2010**, *158*, 1169–1181. [CrossRef] [PubMed]
3. Tang, H.; Hassan, M.; Nawaz, M.; Yang, W.; Liu, Y.; Yang, B. A review on sources of soil antimony pollution and recent progress on remediation of antimony polluted soils. *Ecotoxicol. Environ. Saf.* **2023**, *266*, 115583. [CrossRef] [PubMed]
4. Cai, Z.; Ren, B.; Xie, Q.; Deng, X.; Yin, W.; Chen, L. Potential toxic heavy metals in village topsoil of antimony mining area: Pollution and distribution, environmental safety—A case study of Qilijiang village in xikuangshan mining area, central Hunan Province, China. *Ecol. Indic.* **2023**, *155*, 111033. [CrossRef]
5. Haider, F.; Zulfiqar, U.; Ain, N.; Mehmood, T.; Ali, U.; Ramos Aguila, L.; Li, Y.; Siddique, K.; Farooq, M. Managing antimony pollution: Insights into Soil–Plant system dynamics and remediation Strategies. *Chemosphere* **2024**, *362*, 142694. [CrossRef]
6. He, M.; Wang, X.; Wu, F.; Fu, Z. Antimony pollution in China. *Sci. Total Environ.* **2012**, *421–422*, 41–50. [CrossRef]
7. Bolan, N.; Kumar, M.; Singh, E.; Kumar, A.; Singh, L.; Kumar, S.; Siddique, K. Antimony contamination and its risk management in complex environmental settings: A review. *Environ. Int.* **2022**, *158*, 106908. [CrossRef]
8. Lai, Z.; He, M.; Lin, C.; Ouyang, W.; Liu, X. Interactions of antimony with biomolecules and its effects on human health. *Ecotoxicol. Environ. Saf.* **2022**, *233*, 113317. [CrossRef]
9. Okkenhaug, G.; Gebhardt, K.; Amstaetter, K.; Bue, H.; Herzel, H.; Mariussen, E.; Mulder, J. Antimony (Sb) and lead (Pb) in contaminated shooting range soils: Sb and Pb mobility and immobilization by iron based sorbents, a field study. *J. Hazard. Mater.* **2016**, *307*, 336–343. [CrossRef]
10. Barker, A.; Mayhew, L.; Douglas, T.; Ilgen, A.; Trainor, T. Lead and antimony speciation associated with the weathering of bullets in a historic shooting range in Alaska. *Chem. Geol.* **2020**, *553*, 119797. [CrossRef]
11. Kolbe, F.; Weiss, H.; Morgenstern, P.; Wennrich, R.; Lorenz, W.; Schurk, K.; Stanjek, H.; Daus, B. Sorption of aqueous antimony and arsenic species onto akaganeite. *J. Colloid Interface Sci.* **2011**, *357*, 460–465. [CrossRef]
12. Qi, P.; Pichler, T. Competitive adsorption of As(III), As(V), Sb(III) and Sb(V) onto ferrihydrite in multi-component systems: Implications for mobility and distribution. *J. Hazard. Mater.* **2017**, *330*, 142–148. [CrossRef]
13. Chen, W.; Deng, R.; Chen, Y.; Wang, C.; Hou, B.; Zhou, S.; Hursthouse, A. New insights into adsorption of As(V) and Sb(V) from aqueous by HCO–(Fe3O4)x adsorbent: Adsorption behaviors, competition and mechanisms. *J. Water Process Eng.* **2024**, *58*, 104873. [CrossRef]
14. Gao, Y.; Mucci, A. Acid base reactions, phosphate and arsenate complexation, and their competitive adsorption at the surface of goethite in 0.7 M NaCl solution. *Geochim. Cosmochim. Acta* **2001**, *65*, 2361–2378. [CrossRef]
15. Neupane, G.; Donahoe, R.; Arai, Y. Kinetics of competitive adsorption/desorption of arsenate and phosphate at the ferrihydrite–water interface. *Chem. Geol.* **2014**, *368*, 31–38. [CrossRef]
16. Pintor, A.; Vieira, B.; Brandão, C.; Boaventura, R.; Botelho, C. Complexation mechanisms in arsenic and phosphorus adsorption onto iron-coated cork granulates. *J. Environ. Chem. Eng.* **2020**, *8*, 104184. [CrossRef]
17. Wang, Q.; Zhang, G.; Liu, S.; Mao, K.; Ma, C.; Chen, J.; Liu, F. The impact of phosphate on the interaction of Sb(III) with ferrous sulfide. *Appl. Geochem.* **2022**, *140*, 105297. [CrossRef]
18. Wang, Z.; Ma, X.; Pan, H.; Yang, X.; Zhang, X.; Lyu, Y.; Liao, W.; Shui, W.; Wu, J.; Xu, M.; et al. Investigating effects of phosphogypsum disposal practices on the environmental performance of phosphate fertilizer production using emergy analysis and carbon emission amounting: A case study from China. *J. Clean. Prod.* **2023**, *409*, 137248. [CrossRef]
19. Tong, B.; Xu, H.; Liu, Z. Current global distribution of antimony mineral resources and suggestions for exploration and Investment in China. *China Min. Mag.* **2017**, *26*, 5–10. (In Chinese)
20. Xie, Q.; Ren, B.; Shi, X.; Hursthouse, A. Factors on the distribution, migration, and leaching of potential toxic metals in the soil and risk assessment around the zinc smelter. *Ecol. Indic.* **2022**, *144*, 109502. [CrossRef]
21. Stuckey, J.; Schaefer, M.; Benner, S.; Fendorf, S. Reactivity and speciation of mineral-associated arsenic in seasonal and permanent wetlands of the Mekong Delta. *Geochim. Cosmochim. Acta* **2015**, *171*, 143–155. [CrossRef]
22. Lin, T.; Wei, C.; Huang, C.; Chang, C.; Hsu, F.; Liao, V. Both Phosphorus Fertilizers and Indigenous Bacteria Enhance Arsenic Release into Groundwater in Arsenic-Contaminated Aquifers. *J. Agric. Food Chem.* **2016**, *64*, 2214–2222. [CrossRef] [PubMed]

23. Fathi-Gerdelidani, A.; Towfighi, H.; Shahbazi, K. Kinetic studies on arsenic release from geogenically enriched soils under oxidized and reduced conditions. *J. Geochem. Explor.* **2022**, *242*, 107083. [CrossRef]
24. Lu, R. *Analytical Methods for Soil and Agro-Chemistry*; China Agricultural Science and Technology Press: Beijing, China, 2000; pp. 56–57.
25. Shangguan, Y.; Zhao, L.; Qin, Y.; Hou, H.; Zhang, N. Antimony release from contaminated mine soils and its migration in four typical soils using lysimeter experiments. *Ecotoxicol. Environ. Saf.* **2016**, *133*, 1–9. [CrossRef] [PubMed]
26. Zhang, H.; Li, L.; Zhou, S. Kinetic modeling of antimony(V) adsorption–desorption and transport in soils. *Chemosphere* **2014**, *111*, 434–440. [CrossRef]
27. Wang, X.; Zhang, Y.; Song, C.; Shen, Z.; Wang, T.; Yang, K.; Miao, H.; Yang, J.; Wang, J.; Xu, X. Novel insight into the competitive adsorption behaviors of As(V), Sb(V), and P(V) on {110} facets of Goethite: Existing form and coordination structure affinity. *Chem. Eng. J.* **2024**, *479*, 147677. [CrossRef]
28. Pintor, A.; Brandão, C.; Boaventura, R.; Botelho, C. Multicomponent adsorption of pentavalent As, Sb and P onto iron-coated cork granulates. *J. Hazard. Mater.* **2021**, *406*, 124339. [CrossRef]
29. Fumiaki, K.; Ikuo, A.; Hiroshi, K.; Issaku, U. Fractal model for adsorption on activated carbon surfaces: Langmuir and Freundlich adsorption. *Surf. Sci.* **2000**, *467*, 131–138. [CrossRef]
30. Passé-Coutrin, N.; Sandro, A.; Sarra, G. Assessment of the surface area occupied by molecules on activated carbon from liquid phase adsorption data from a combination of the BET and the Freundlich theories. *J. Colloid Interface Sci.* **2009**, *332*, 515–519. [CrossRef]
31. Kundu, S.; Gupta, A. Arsenic adsorption onto iron oxide-coated cement (IOCC): Regression analysis of equilibrium data with several isotherm models and their optimization. *Chem. Eng. J.* **2006**, *122*, 93–106. [CrossRef]
32. Wu, D.; Sun, S.; He, M.; Wu, Z.; Xiao, J.; Chen, X.; Wu, W. As(V) and Sb(V) co-adsorption onto ferrihydrite: Synergistic effect of Sb(V) on As(V) under competitive conditions. *Environ. Sci. Pollut. Res.* **2018**, *25*, 14585–14594. [CrossRef] [PubMed]
33. Waltham, C.; Eick, M. Kinetics of arsenic adsorption on goethite in the presence of sorbed silicic acid. *Soil. Sci. Soc. Am. J.* **2002**, *66*, 818–825. [CrossRef]
34. Martinez-Llado, X.; Valderrama, C.; Rovira, M.; Marti, V.; Gimenez, J.; de Pablo, J. Sorption and mobility of Sb(V) in calcareous soils of Catalonia (NE Spain): Batch and column experiments. *Geoderma* **2011**, *160*, 468–476. [CrossRef]
35. Zhao, H.; Robert, S. Competitive Adsorption of Phosphate and Arsenate on Goethite. *Environ. Sci. Technol.* **2001**, *35*, 4753–4757. [CrossRef]
36. McComb, K.; Craw, D.; McQuillan, A. ATR-IR spectroscopic study of antimonate adsorption to iron oxide. *Langmuir* **2007**, *23*, 12125–12130. [CrossRef]
37. Griggs, C.; Martin, W.; Larson, S.; O'Connnor, G.; Fabian, G.; Zynda, G.; Mackie, D. The effect of phosphate application on the mobility of antimony in firing range soils. *Sci. Total Environ.* **2011**, *409*, 2397–2403. [CrossRef]
38. Zhang, X.; Chen, J.; Ye, T.; Yi, H.; Lei, S.; Cui, X.; Luo, D.; Xiao, T.; Cui, J. Iron and phosphate species regulates arsenic speciation and potential mobility in contaminated soils. *J. Geochem. Explor.* **2025**, *268*, 107610. [CrossRef]
39. Tsuchida, K.; Nakamura, K.; Watanabe, N.; Komai, T. Influence of non-uniform flow on toxic elements transport in soil column percolation test. *Heliyon* **2022**, *8*, 11541. [CrossRef]

Disclaimer/Publisher's Note: The statements, opinions and data contained in all publications are solely those of the individual author(s) and contributor(s) and not of MDPI and/or the editor(s). MDPI and/or the editor(s) disclaim responsibility for any injury to people or property resulting from any ideas, methods, instructions or products referred to in the content.